1

Beam shaping to improve the free-electron laser performance at the Linac Coherent Light Source

Y. Ding and M. Guetg

SLAC National Accelerator Laboratory, Menlo Park, California 94025, USA

A new operating mode has been developed for the Linac Coherent Light Source (LCLS) in which we shape the longitudinal phase space of the electron beam. This mode of operation is realized using a horizontal collimator located in the middle of the first bunch compressor to truncate the head and tail of the beam. With this method, the electron beam longitudinal phase space and current profile are re-shaped, and improvement in lasing performance can be realized. Combined with correction of the beam tilt induced from coherent syncrotron radiation in bending magnets, a high-peak-power operating mode with over 200 GW has been demonstrated at the LCLS using the reshaped beam.

1. Introduction

Over the past several years, great progress has been made in the realization of high power x-ray free-electron lasers (FELs). This revolutionary light source, with 8-10 orders increase in peak brightness and 2-3 orders decrease in pulse length compared to the pulses from storage ring-based third generation light source, provides an unique tool for ultrafast x-ray studies with atomic spatial resolution [1,2]. Nevertheless, there is a continual desire for x-ray pulses with further improved brightness and peak power, driven by x-ray users with applications such as single-molecule imaging [3] and nonlinear x-ray sciences [4]. In a linac-driven FEL, the FEL lasing performance mainly depends on the electron beam brightness, where a combination of low transverse emittance, high peak current and small energy spread are desired.

The final electron beam time-sliced emittance is mostly determined in the photoinjector located at the very beginning of the facility. The energy spread is typically controlled by a laser heater (see example at the Linac Coherent Light Source (LCLS) [5,6]), which is designed to suppress the microbunching instability and yet achieve a small final slice energy spread. This laser heater "knob" can be easily adjusted during operation for maximizing the FEL photon output. The beam peak current, enhanced by longitudinal compression, however is one complicated parameter for optimization since collective effects are involved during the bunch compression, and the non-uniform current profile after compression also causes additional beam brightness degradation in the downstream beamline. We will focus on shaping the current profile in this paper.

In the linac section, the bunch is compressed in a series of magnetic chicanes in order to achieve a high peak current. To do this, the electron beam is accelerated at an off-crest radio-frequency (rf) phase so that the bunch tail has higher energy than

2

the head. While passing through a four-dipole chicane, the tail travels a shorter path than the head, thus catching up to the head and compressing the bunch in time. The nonlinearities induced by the acceleration and compression processes (e.g., by the longitudinal wakefields, rf curvature, and second order momentum compaction) need to be minimized to avoid high peak current spikes in the temporal distributions[7]. In addition, collective effects such as coherent synchrotron radiation (CSR) in the dipoles can cause significant time-dependent energy loss and projected emittance growth[8]. The nonlinearities and the CSR effect are major issues that limit the peak currents that can be achieved.

In a recent paper[9], we reported a study at the LCLS with a beam shaping technique, which is realized by truncating the double-horn current spikes (at the beam head and tail) with a collimator located at the middle of a bunch compressor. Experimental results have demonstrated that collimation is a robust method for manipulating the current profile and final longitudinal phase space. A flat-top-like current profile with reduced current spikes has been achieved, one that leads to better FEL performance with improved pulse energy, peak power and bandwidth control. We will summarize the horn-collimation-based beam shaping studies first, and then discuss a high-power mode with CSR correction using the collimated beam[15,16].

2. Beam shaping with a collimation

The longitudinal collimation method[9] relies upon the fact that a time-energy chirped beam is tilted at a large angle relative to the longitudinal axis in a dispersive section. For example, at the middle of a magnetic chicane where the maximum tilt exists, cutting the beam edges horizontally with a transverse collimator is effectively truncating the bunch head and tail.
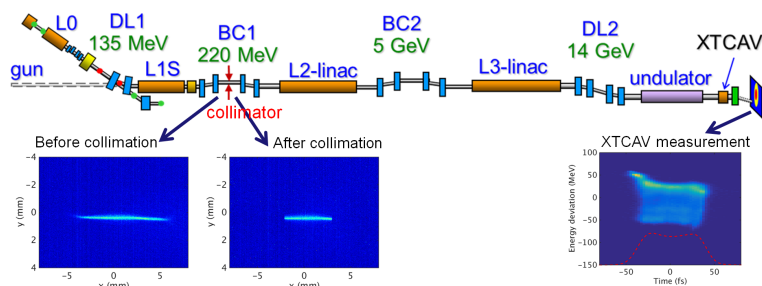
Fig. 1. A schematic of the LCLS machine layout including a collimator in the middle of the first bunch compressor (BC1) and the XTCAV downstream of the FEL undulator. The L2 and L3 are S-band RF linac sections. We also show the measured images at the middle of the BC1, before and after collimation, and a measured example from XTCAV for the collimated beam after FEL lasing[9].

The longitudinal collimation mode was also studied as a beam slice diagnostic

at the Fermi FEL [10] and the LCLS[11]. As discussed in [10], this also has the potential to generate shorter x-ray pulses by truncating most of the charge, with only a small fraction of the bunch passing through the collimator gap. Compared with a low-charge operation mode [12], the collimated beam will have a larger emittance since it starts with a higher charge in the electron gun. However, this collimation mode provides a simple way to shape the electron beam's phase space by truncating a small fraction of the charge at the bunch head and tail [11]. For the beam shaping purpose as studied in this paper, we still keep most of the bunch charge and only scrape away a small number of the unwanted particles.

At the LCLS, both the first and second bunch compressor (BC1 and BC2 in Fig. 1) have a horizontal collimator at the middle of the chicane. Considering radiation protection issues, we choose the low-energy chicane BC1, where the regular operating energy is 220 MeV, for collimation. The machine layout is shown in Fig. 1. The collimator and chicane parameters have been discussed in [11]. For example, at the BC1 collimator location, the horizontal dispersion is 0.23 m, and the rms energy spread is typically about 1%. Thus the horizontal full width of a dispersed beam at the collimator is about 11 mm. Under typical collimating conditions during operation, the collimator gap at the LCLS is set to a full width of 5 - 7 mm, from which the bunch charge is truncated from initial 250 pC to about 180 pC. At the bottom of Fig. 1, we include measured examples of the beam on an optical transition radiation (OTR) screen in the middle of BC1, without collimation and with collimation; and an example of the final beam's longitudinal distribution measured at the end of the undulator with the collimation mode. With this setup, the current profile after BC1 has sharp edges and the downstream L2-linac wakefield induced energy loss is getting linear, which helps suppress the current horns in BC2 compression [9].

We use a hard x-ray FEL example (photon energy of 7 keV) to discuss the lasing performance with a collimated beam. We list the major machine parameters in Table 1. The charge is truncated by the BC1 collimator from 250 pC to 180 pC. An X-band transverse deflector (XTCAV) [13], located downstream of the undulator section, provides a direct measured of the beam longitudinal phase space. In addition, since the location of the measurement is downstream of the FEL lasing process, the lasing induced time-resolved energy loss or energy spread growth can also be measured. By comparing with lasing-off images (suppress the lasing with an oscillating orbit inside the undulator beamline) one can reconstruct the FEL power profile [14].

Figure 2 (a) and (b) show measured examples of the collimated beam longitudinal phase space with lasing-off and lasing-on conditions. The electron beam current profile and reconstructed x-ray power profile are shown in (c). We see in this example, the peak current is about 2.5 kA with a relatively uniform profile, which agrees well with the simulation predictions. Since the current profile and the longitudinal phase space are getting uniform, we can see that a uniform lasing along the bunch

4
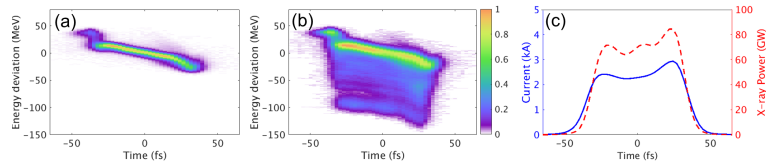
Fig. 2. Measurement examples of the collimated beam for hard x-ray FEL case with photon energy 7 keV[9]. The electron beam energy is 12.5 GeV, and other machine parameters can be found in Table 1. The electron beam longitudinal phase space is shown in (a) for lasing-off condition and (b) for lasing-on condition; in (c) the beam current profile and reconstructed FEL power profile are given. In this example the x-ray pulse energy is 4.8 mJ.

Parameter	Symbol	Value	Unit
Bunch charge at injector	Q_0	250	pC
Bunch charge after BC1	Q	180	pC
Beam energy at BC1	E_1	220	MeV
Beam energy at BC2	E_2	5	GeV
Beam final energy	E_f	12.5	GeV
BC1 current	I_1	220	A
BC2 current	I_2	3-5	kA
BC1 collimator gap	g	~ 6	mm
BC1 R56		-45.5	mm
BC2 R56		-28	mm

can be achieved, producing a pulse energy over 4 mJ in a routine operation at this energy. The x-ray peak power ranges from 50 to 100 GW depending on the pulse duration.

3. High power FELs with CSR correction

For FEL operation, higher current leads to a higher saturation power. However, stronger CSR effect shows up during the bunch compression and other dog-leg area. CSR leads to a longitudinally dependent energy loss along the bunch. The subsequent bends translate this energy difference to a transverse misalignment of the longitudinal slices of the bunch, expressed by the beam yaw. Yawed beams affect the FEL performance negatively because of nonuniform lasing. A recent paper[15] based on theory and simulations proposed a method to remove the beam yaw by the careful control of the dispersion at locations with a strong energy chirp using multipole magnets.

Experimental studies at the LCLS with adopting the CSR correction with dispersion control showed encouraging improvement for the FEL power[16]. In this study, we truncated more charge on the bunch head and tail with about half of the charge left. In this way, a better time-energy linearity on the beam allows stronger compression in the second bunch compressor, and also leads to less higher-order

beam yaws. We measured a current of over 6 kA in the second bunch compressor, well above the standard operating point about 3-4 kA. Then we used the existing tweaker quadrupoles inside the compressor and DL2 to correct the beam yaw.

We show in Fig. 3 two measurement examples of the high-power FEL pulse [16]. The electron beam energy is 12 GeV with photon energy 6.6 keV. In the two examples the peak power is about 300 GW with pulse duration about 10 fs. Averaging over thousand shots, the peak power is still over 200 GW.
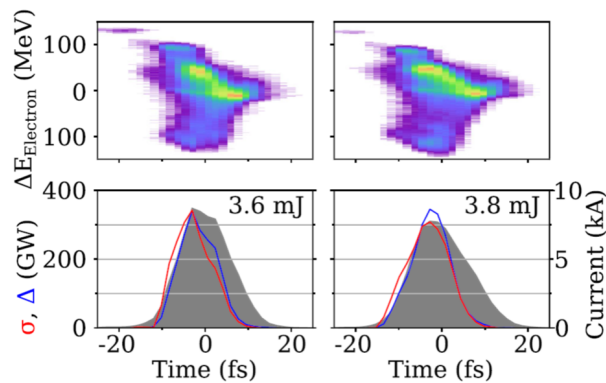
Fig. 3. Measurement examples of high-power FELs [16]. Top: longitudinal phase space after lasing; Bottom: FEL pulse power calculated by energy loss or energy spread, and current profile.

4. Summary

We have developed a new operating mode with longitudinal beam shaping for improving the FEL performance at the LCLS. This is based on the existing hardware and can be easily applied to other accelerator facilities using normal conducting rf. With a more uniform current distribution after truncating the head/tail horns, some collective effects such as CSR, space charge and wakefields are reduced. This greatly helps transverse matching and FEL optimization, and makes it possible for high-current operatoin. We have demonstrated at the LCLS that with the electron beam current over 6 kA, the FEL peak power can be achieved over 200 GW with CSR tilt correction using dispersion control.

5. Acknowledgments

6

References

1. Zhirong Huang and Kwang-Je Kim. Review of x-ray free-electron laser theory. *Phys. Rev. ST Accel. Beams*, 10:034801, Mar 2007.

2. B. W. J. McNeil and N. R. Thompson. X-ray free-electron lasers. *Nat. Photon.*, 4:814, 2010.

3. A. Aquila, A. Barty, C. Bostedt, S. Boutet, G. Carini, D. dePonte, P. Drell, S. Doniach, K. H. Downing, T. Earnest, H. Elmlund, V. Elser, M. Ghr, J. Hajdu, J. Hastings, S. P. Hau-Riege, Z. Huang, E. E. Lattman, F. R. N. C. Maia, S. Marchesini, A. Ourmazd, C. Pellegrini, R. Santra, I. Schlichting, C. Schroer, J. C. H. Spence, I. A. Vartanyants, S. Wakatsuki, W. I. Weis, and G. J. Williams. The linac coherent light source single particle imaging road map. *Structural Dynamics*, 2(4), 2015.

4. R. W Schoenlei and et al. New science opportunities enabled by LCLS-II x-ray lasers. *SLAC Report SLAC-R-1053*, 2015.

5. Z. Huang, M. Borland, P. Emma, J. Wu, C. Limborg, G. Stupakov, and J. Welch. Suppression of microbunching instability in the linac coherent light source. *Phys. Rev. ST Accel. Beams*, 7:074401, Jul 2004.

6. Z. Huang, A. Brachmann, F.-J. Decker, Y. Ding, D. Dowell, P. Emma, J. Frisch, S. Gilevich, G. Hays, Ph. Hering, R. Iverson, H. Loos, A. Miahnahri, H.-D. Nuhn, D. Ratner, G. Stupakov, J. Turner, J. Welch, W. White, J. Wu, and D. Xiang. Measurements of the linac coherent light source laser heater and its impact on the x-ray free-electron laser performance. *Phys. Rev. ST Accel. Beams*, 13:020703, Feb 2010.

7. J. Arthur and et al. *Linac Coherent Light Source (LCLS) Conceptual Design Report*, SLAC-R-593, 2002.

8. K. L. F. Bane, F.-J. Decker, Y. Ding, D. Dowell, P. Emma, J. Frisch, Z. Huang, R. Iverson, C. Limborg-Deprey, H. Loos, H.-D. Nuhn, D. Ratner, G. Stupakov, J. Turner, J. Welch, and J. Wu. Measurements and modeling of coherent synchrotron radiation and its impact on the linac coherent light source electron beam. *Phys. Rev. ST Accel. Beams*, 12:030704, Mar 2009.

9. Y. Ding, K. L. F. Bane, W. Colocho, F.-J. Decker, P. Emma, J. Frisch, M. W. Guetg, Z. Huang, R. Iverson, J. Krzywinski, H. Loos, A. Lutman, T. J. Maxwell, H.-D. Nuhn, D. Ratner, J. Turner, J. Welch, and F. Zhou. Beam shaping to improve the free-electron laser performance at the linac coherent light source. *Phys. Rev. Accel. Beams*, 19:100703, Oct 2016.

10. S. Di Mitri, D. Castronovo, I. Cudin, and L. Fröhlich. Electron slicing for the generation of tunable femtosecond soft x-ray pulses from a free electron laser and slice diagnostics. *Phys. Rev. ST Accel. Beams*, 16:042801, Apr 2013.

11. F. Zhou, K. Bane, Y. Ding, Z. Huang, H. Loos, and T. Raubenheimer. Measurements and analysis of a high-brightness electron beam collimated in a magnetic bunch compressor. *Phys. Rev. ST Accel. Beams*, 18:050702, May 2015.

12. Y Ding, A Brachmann, F-J Decker, D Dowell, P Emma, J Frisch, S Gilevich, G Hays, Ph Hering, Z Huang, et al. Measurements and simulations of ultralow emittance and ultrashort electron beams in the linac coherent light source. *Physical review letters*, 102(25):254801, 2009.

13. C. Behrens, F-J Decker, Y Ding, VA Dolgashev, J Frisch, Z Huang, P Krejcik, H Loos, A Lutman, TJ Maxwell, et al. Few-femtosecond time-resolved measurements of x-ray free-electron lasers. *Nature communications*, 5:3762, 2014.

14. Y. Ding, C. Behrens, P. Emma, J. Frisch, Z. Huang, H. Loos, P. Krejcik, and M-H. Wang. Femtosecond x-ray pulse temporal characterization in free-electron lasers using a transverse deflector. *Phys. Rev. ST Accel. Beams*, 14:120701, Dec 2011.

15. Marc Walter Guetg, Bolko Beutner, Eduard Prat, and Sven Reiche. Optimization of

7

free electron laser performance by dispersion-based beam-tilt correction. *Phys. Rev. ST Accel. Beams*, 18:030701, Mar 2015.

16. Marc W. Guetg, Alberto A. Lutman, Yuantao Ding, Timothy J. Maxwell, Franz-Josef Decker, Uwe Bergmann, and Zhirong Huang. Generation of high-power high-intensity short x-ray free-electron-laser pulses. *Phys. Rev. Lett.*, 120:014801, Jan 2018.